Electronic Supplementary Material (ESI) for Soft Matter.

Equilibrium shapes of a twist-bend nematic drop

Kanakapura S. Krishnamurthy,[a] Pramoda Kumar,[b] Nani B. Palakurthy,[a] Channabasaveshwar V. Yelamaggad,[a] and Epifanio G. Virga*[c]

These notes supplement our paper *Interfacial and morphological features of a twist-bend nematic drop*, producing a number of analytical details of the mathematical model employed there to interpret the experimental observations of equilibrium shapes of a twist-bend nematic drop in two space dimensions. For the sake of continuity and completeness, some figures and equations are also reproduced here.

1 Equilibrium equations

Our starting point here is the energy functional

$$F[\boldsymbol{r}] := \int_0^L \left\{1+\frac{1}{2}\omega\left[(\boldsymbol{t}\cdot\boldsymbol{n})^2-c^2\right]^2\right\}ds, \tag{1}$$

where L is the (undetermined) length of the curve $\mathscr{C}$ bounding the drop, $\boldsymbol{t}$ is a unit tangent vector to $\mathscr{C}$, and s is the corresponding arc-length co-ordinate, so that $\mathscr{C}$ is described by the mapping $s \mapsto \boldsymbol{r}(s)$ and $\boldsymbol{t} = \boldsymbol{r}'$, where a prime $'$ denotes differentiation with respect to s.

Figure 1a illustrates an admissible shape for $\mathscr{C}$, symmetric with respect to both axes x and y, the former designating the orientation of $\boldsymbol{n}$. The area A enclosed by $\mathscr{C}$ can be expressed in terms of $\boldsymbol{r}$ as

$$A[\boldsymbol{r}] := -\frac{1}{2}\int_0^L \boldsymbol{r}\times\boldsymbol{t}\cdot\boldsymbol{e}_z ds, \tag{2}$$

where $\boldsymbol{e}_z := \boldsymbol{e}_x \times \boldsymbol{e}_y$.

Constrained equilibrium for F requires that $\boldsymbol{r}$ makes the first variations δF and δA proportional to one another,

$$\delta F = \lambda\delta A, \tag{3}$$

where λ is a Lagrange multiplier, still to be determined. The first variation δF is a functional, $\delta F(\boldsymbol{r})[\boldsymbol{u}]$, linear in the variation $\boldsymbol{u}$ of $\boldsymbol{r}$. Formally,

$$\delta F(\boldsymbol{r})[\boldsymbol{u}] := \left.\frac{d}{ds}F[\boldsymbol{r}_\varepsilon]\right|_{\varepsilon=0}, \tag{4}$$

where $\boldsymbol{r}_\varepsilon := \boldsymbol{r}+\varepsilon\boldsymbol{u}$ and ε is a small, perturbation parameter. The perturbed curve $\mathscr{C}_\varepsilon$ described by $\boldsymbol{r}_\varepsilon$ has unit tangent vector $\boldsymbol{t}_\varepsilon$ delivered by

$$\boldsymbol{t}_\varepsilon = \boldsymbol{t}+\varepsilon(\mathbf{I}-\boldsymbol{t}\otimes\boldsymbol{t})\boldsymbol{u}'+o(\varepsilon), \tag{5}$$

where $\mathbf{I}$ is the identity tensor. Moreover, the local dilation ratio between lengths along $\mathscr{C}_\varepsilon$ and lengths along $\mathscr{C}$ is, to within first order in ε, $1+\varepsilon\boldsymbol{t}\cdot\boldsymbol{u}'$. Thus, by letting $\boldsymbol{n}=\boldsymbol{e}_x$ from (1) and (4) we obtain

$$\begin{aligned}\delta F(\boldsymbol{r})[\boldsymbol{u}] = \int_0^L &\left\{2\omega\left[(\boldsymbol{t}\cdot\boldsymbol{e}_x)^2-c^2\right](\mathbf{I}-\boldsymbol{t}\otimes\boldsymbol{t})\boldsymbol{e}_x\right.\\ &\left.+\left(1+\frac{1}{2}\omega\left[(\boldsymbol{t}\cdot\boldsymbol{e}_x)^2-c^2\right]^2\right)\boldsymbol{t}\right\}\cdot\boldsymbol{u}'ds.\end{aligned} \tag{6}$$

Similarly, we arrive at

$$\delta A(\boldsymbol{r})[\boldsymbol{u}] = \frac{1}{2}\int_0^L(\boldsymbol{\nu}\cdot\boldsymbol{u}-\boldsymbol{e}_z\times\boldsymbol{r}\cdot\boldsymbol{u}')\,ds, \tag{7}$$

where $\boldsymbol{\nu} := \boldsymbol{e}_z\times\boldsymbol{t}$ is the outer unit normal to $\mathscr{C}$.

As shown in Fig. 1a, $\mathscr{C}$ may possess a *corner*, that is a point, say at $s=s_0$, where the unit tangent $\boldsymbol{t}$ jumps from $\boldsymbol{t}^-$ to $\boldsymbol{t}^+$ as s increases through s_0. If this is the case, splitting the integral in (7) into subintervals where $\boldsymbol{t}$ is continuous, allowing both $\boldsymbol{u}$ and $\boldsymbol{u}'$ to be everywhere continuous, and integrating by parts, we easily show that

$$\delta A(\boldsymbol{r})[\boldsymbol{u}] = \int_0^L \boldsymbol{\nu}\cdot\boldsymbol{u}ds. \tag{8}$$

Contrariwise, proceeding just in the same way, we extract a *jump* contribution to $\delta F(\boldsymbol{r})$ from every point of discontinuity for $\boldsymbol{t}$, which reads as $[\![\boldsymbol{f}]\!]\cdot\boldsymbol{u}$, where

$$\begin{aligned}\boldsymbol{f} := &\,2\omega[(\boldsymbol{t}\cdot\boldsymbol{e}_x)^2-c^2](\boldsymbol{t}\cdot\boldsymbol{e}_x)(\mathbf{I}-\boldsymbol{t}\otimes\boldsymbol{t})\boldsymbol{e}_x\\ &+\left(1+\frac{1}{2}\omega[(\boldsymbol{t}\cdot\boldsymbol{e}_x)^2-c^2]^2\right)\boldsymbol{t}\end{aligned} \tag{9}$$

and, as customary, for any discontinuous field ψ the *jump* $[\![\psi]\!]$ is defined by $[\![\psi]\!] := \psi^+-\psi^-$, where ψ^+ and ψ^- are the right and left limits of ψ at the point of discontinuity.

Requiring (3) to be valid for arbitrary $\boldsymbol{u}$, by (6) and (8) we conclude that the equilibrium equation for the regular arcs of $\mathscr{C}$, where $\boldsymbol{t}$ is continuous, is

$$\boldsymbol{f}'+\lambda\boldsymbol{\nu} = \boldsymbol{0}, \tag{10}$$

[a] *Centre for Nano and Soft Matter Sciences, P. O. Box 1329, Jalahalli, Bangalore 560013, India. E-mail: murthyksk@gmail.com*
[b] *The Jacob Blaustein Institutes for Desert Research, Ben-Gurion University of the Negev, Sede Boqer Campus, Israel 8499000.*
[c] *Dipartimento di Matematica, Università di Pavia, Via Ferrata 5, I-27100 Pavia, Italy. E-mail: eg.virga@unipv.it*

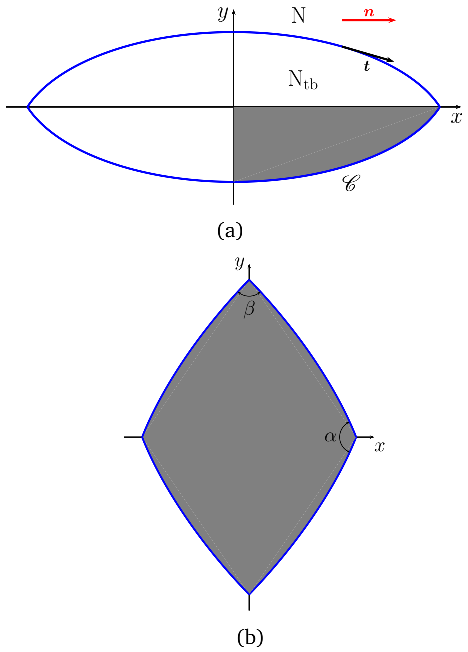

Fig. 1: (a) An admissible curve $\mathscr{C}$ with a two-fold symmetry. The symmetry axis x designates the orientation of the uniformly aligned nematic phase, N. The region delimited by $\mathscr{C}$ is occupied by the $\mathrm{N_{tb}}$ phase; $\boldsymbol{t}$ is the tangent unit vector to $\mathscr{C}$, to be identified with the twist director on the drop's interface. The specific curve $\mathscr{C}$ depicted here has a corner where it meets the x axis, whereas it is smooth where it meets the y axis. The gray quarter, which by repeated reflections covers the whole drop, admits a Cartesian representation, $y = y(x)$. (b) A two-fold symmetric shape exhibiting four corners on the symmetry axes; α and β are the corresponding inner corner angles.

while the equation

$$[\![\boldsymbol{f}]\!] = \mathbf{0} \tag{11}$$

must hold at all corners, where $\boldsymbol{t}$ is discontinuous. These are precisely equations (8) and (9) in our main paper.

2 Equilibrium corners

In general, the equilibrium equations (10) and (11) are rather complicated. Symmetry may simplify them. In keeping with the experimental observations, we shall hereafter assume that $\mathscr{C}$ has the two-fold symmetry displayed in Fig. 1 and that its corners may only occur on the symmetry axes.

For a corner on the y axis, $\boldsymbol{t}^-$ and $\boldsymbol{t}^+$ satisfy

$$\boldsymbol{t}^+ \cdot \boldsymbol{e}_x = \boldsymbol{t}^- \cdot \boldsymbol{e}_x, \quad \boldsymbol{t}^+ \cdot \boldsymbol{e}_y = -\boldsymbol{t}^- \cdot \boldsymbol{e}_y, \tag{12}$$

and it can be shown that equation (11) reduces to

$$3\omega\chi^2 - 2\omega c^2\chi - 2 - \omega c^4 = 0, \tag{13}$$

where we have set $\chi := (\boldsymbol{t} \cdot \boldsymbol{e}_x)^2$. It can be easily proved that there is precisely one root of (13) in $[0, 1]$, which reads

$$\chi = \chi_1(c, \omega) := \frac{1}{3}\left(c^2 + \sqrt{4c^4 + \frac{6}{\omega}}\right), \tag{14}$$

if and only if

$$\omega \geqq \omega_{\mathrm{c}}^{(1)}(c) := \frac{2}{(1 - c^2)(3 + c^2)}. \tag{15}$$

Otherwise, there is none and at equilibrium no corner can arise where $\mathscr{C}$ meets the y axis. The inner corner angle β depicted in Fig. 1b is given by

$$\beta = 2 \arcsin \sqrt{\chi_1}, \tag{16}$$

where χ_1 is as in (14); in particular, (16) implies that

$$\lim_{\omega \to \infty} \beta(c, \omega) = 2 \arcsin c. \tag{17}$$

Similarly, for a corner on the x axis,

$$\boldsymbol{t}^+ \cdot \boldsymbol{e}_x = -\boldsymbol{t}^- \cdot \boldsymbol{e}_x, \quad \boldsymbol{t}^+ \cdot \boldsymbol{e}_y = \boldsymbol{t}^- \cdot \boldsymbol{e}_y \tag{18}$$

and (11) reduces to

$$3\omega\chi^2 - 2\omega(c^2 + 2)\chi - (\omega c^4 - 4\omega c^2 + 2) = 0. \tag{19}$$

It can be easily proved that there is precisely one admissible root of (19), which reads

$$\chi = \chi_2(c, \omega) := \frac{1}{3}\left(c^2 + 2 - \sqrt{4(1 - c^2)^2 + \frac{6}{\omega}}\right), \tag{20}$$

if and only if

$$\omega \geqq \omega_{\mathrm{c}}^{(2)}(c) := \frac{2}{c^2(4 - c^2)}. \tag{21}$$

Otherwise, there is none and at equilibrium no corner can arise where $\mathscr{C}$ meets the x axis. The inner corner angle α depicted in Fig. 1b is given by

$$\alpha = 2 \arccos \sqrt{\chi_2}, \tag{22}$$

where χ_2 is as in (20); in particular, (22) implies that

$$\lim_{\omega \to \infty} \alpha(c, \omega) = 2 \arccos c = 2\vartheta, \tag{23}$$

where ϑ is the ideal cone angle.

The graphs of both $\omega_{\mathrm{c}}^{(1)}$ and $\omega_{\mathrm{c}}^{(2)}$ as functions of c are plotted in Fig. 2.

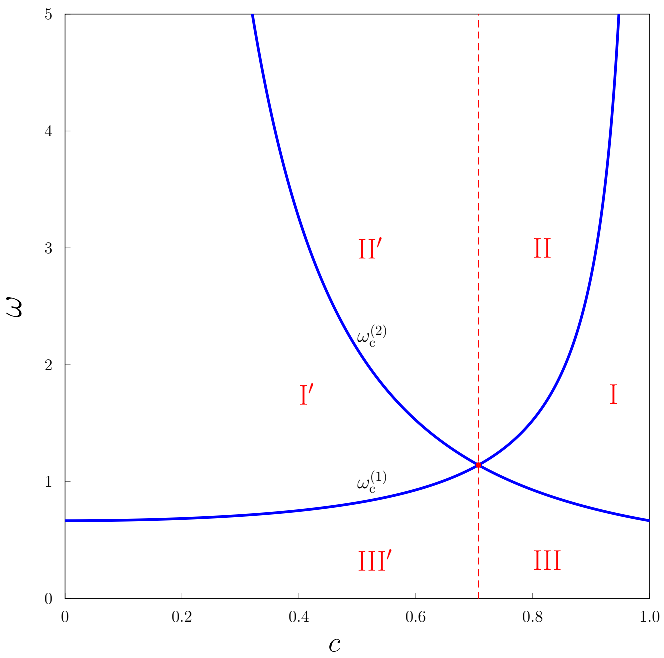

Fig. 2: Phase diagram in the plane (c, ω). Regions I, II, and III ranging over $\frac{1}{\sqrt{2}} \leqq c \leqq 1$ are delimited by the graphs of the functions $\omega_c^{(1)}$ and $\omega_c^{(2)}$ in (15) and (21). These graphs, which cross at the (red) triple point $(\frac{1}{\sqrt{2}}, \frac{8}{7})$, are transformed one into the other by the mapping $c \mapsto \sqrt{1-c^2}$. The corresponding images I′, II′, and III′ of regions I, II, and III, on the other side of the dashed separatrix $c = \frac{1}{\sqrt{2}}$, cover together with I, II, and III the whole admissible parameter plane (c, ω). The equilibrium shape of the drop has no corners in III, but has two and four symmetric corners in I and II, respectively. All transitions from one region to an adjacent region take place continuously: they are *second-order*.

3 Equilibrium arcs

To arrive at a tractable form of the equilibrium equation in (10) for the regular arcs of $\mathscr{C}$, we found it convenient to describe a quarter of a doubly symmetric curve $\mathscr{C}$ as in Fig. 1a in the form of a Cartesian graph $y = y(x)$. With $\mathscr{C}$ thus reparameterized, the functional F in (1) subject to the constraint of the area enclosed by $\mathscr{C}$ can equivalently be rewritten as

$$F^*[y] := \int_0^a \left\{ \left[1 + \frac{1}{2}\omega \left(\frac{1}{1+y'^2} - c^2 \right)^2 \right] \sqrt{1+y'^2} + \lambda y \right\} dx, \tag{24}$$

which has also absorbed the area functional A and the Lagrange multiplier λ associated with it. In (24), a prime now denotes differentiation with respect to x and the function $y(x)$ is subject to

$$y(a) = 0, \tag{25}$$

where $a > 0$ is to be determined.

Since we have already obtained the geometric conditions valid at the equilibrium corners of $\mathscr{C}$, here we are only interested in finding the equilibrium arcs of $\mathscr{C}$ in their Cartesian parametrization. The Euler-Lagrange equation associated with F^* is easily obtained and integrated once, leading to

$$\Phi(y'; c, \omega) = \lambda x + b, \tag{26}$$

where

$$\Phi(u; c, \omega) := \frac{1}{2} \frac{1}{\sqrt{(1+u^2)^5}} \big[2 - 3\omega + 2\omega c^2 + \omega c^4 + 2(2 + \omega c^2 + \omega c^4) u^2 + (2 + \omega c^4) u^4 \big] u \tag{27}$$

and b is an arbitrary integration constant. Altering both x and y by the same factor, say μ, so as to produce a homothetic dilation (or contraction) of $\mathscr{C}$ does not alter the left side of (26). Consequently, λ must be changed into λ/μ for $\mathscr{C}$ to remain an equilibrium curve. This shows that λ can be determined (and the area constraint can be satisfied) by simply rescaling any solution $y = y(\xi)$ of (26) with $\xi := \lambda x + b$. Similarly, since the differential equation (26) does not contain y explicitly, the constraint (25) can be satisfied by translating in space a solution.

Figure 3 illustrates a graphical argument to integrate (26). For an arbitrary ξ, the light gray area represents the integral of y' in ξ; such an area can be obtained by subtracting the dark gray area which represents the integral of Φ in u from the whole area $u\Phi(u)$ of the rectangle delimited by the coordinate lines through (u, ξ). Thus, to within additive constants to be chosen so as to adjust the solution to the geometric constraint, a regular arc of $\mathscr{C}$ can be represented in the parametric form

$$y = Y(u; c, \omega) := u\Phi(u; c, \omega) - \Psi(u; c, \omega), \tag{28a}$$

$$\xi = \Phi(u; c, \omega), \tag{28b}$$

where Ψ is the primitive of Φ in u. It is easily seen that, for a regular arc with $x > 0$ and $y < 0$ as shown in Fig. 1, Y can be given the following explicit representation

$$Y(u; c, \omega) = -\frac{1}{2} \frac{1}{\sqrt{(1+u^2)^5}} [2 + \omega - 2\omega c^2 + \omega c^4 + 2(2 + 2\omega - 3\omega c^2 + \omega c^4) u^2 + (2 - 4\omega c^2 + \omega c^4) u^4]. \tag{29}$$

With the aid of (27) and (29), by direct inspection one easily sees that the functions Φ and Y enjoy the following

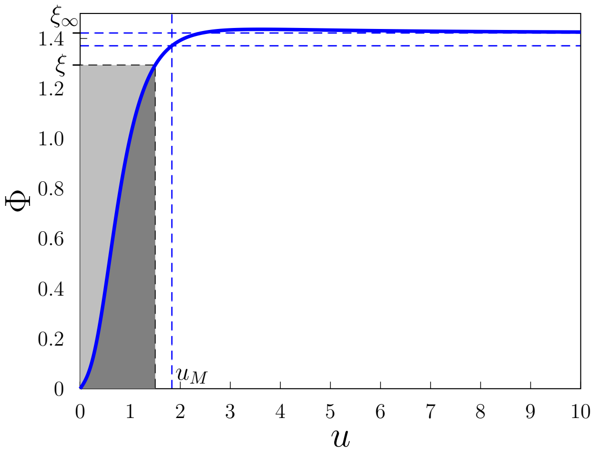

Fig. 3: The plot of the function Φ against u for (c, ω) in region I of the phase diagram in Fig. 2. The asymptote ξ_∞ is delivered by (32); the single value u_M of y' where a regular arc of $\mathscr{C}$ may meet a corner on the x axis is identified by (31). This specific plot, while typical of the whole region I, was obtained for $c = \frac{\sqrt{3}}{2}$ and $\omega = \frac{3}{2}$.

property,

$$\Phi\left(\frac{1}{u}; \sqrt{1-c^2}, \omega\right) = Y(u; c, \omega), \tag{30}$$

which combined with (28) mean that changing c into $\sqrt{1-c^2}$ exchanges ξ with y.

As shown in Fig. 3, in region I a regular arc of $\mathscr{C}$ can extend from $\xi = 0$, where $y' = 0$, to $\xi = \Phi(u_M)$, where $y' = u_M$, with u_M related to χ_2 in (20) through

$$u_M := \sqrt{\frac{1}{\chi_2} - 1}. \tag{31}$$

At $\xi = \Phi(u_M)$, it meets an equilibrium corner on the x axis, whereas it meets none on the y axis. In principle, nothing would prevent one from further extending a regular arc for $\xi > \Phi(u_M)$, but as soon as ξ crosses the asymptote of Φ at

$$\xi_\infty := 1 + \frac{1}{2}\omega c^4, \tag{32}$$

two distinct values of y' can be associated with one and the same ξ in equilibrium, a multiplicity compatible only with a corner of $\mathscr{C}$ away from the symmetry axes, a case that here we have excluded from our consideration as we reckon it likely that these shapes would be metastable. Thus, in region I all equilibrium shapes of $\mathscr{C}$ considered here have two symmetric corners on the x axis [see Fig. 17a in the main paper]; they are tactoids with axis along the direction of nematic alignment outside the drop.

In completely the same fashion, we analyze the equilibrium shape of $\mathscr{C}$ in region II. Figure 4 illustrates the typical appearance of the graph of Φ in such a region. Here u_m, which is related to χ_1 in (14) through

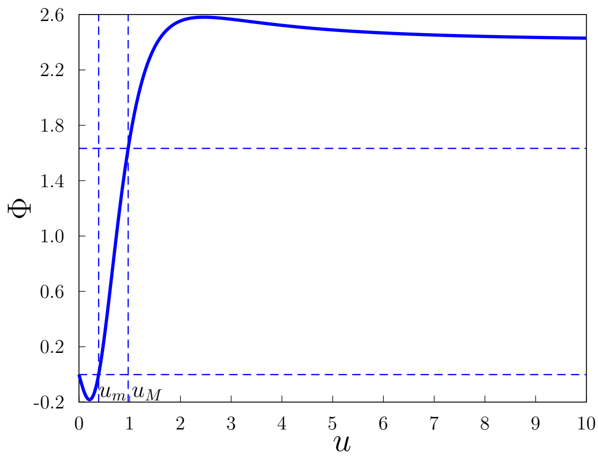

Fig. 4: The plot of the function Φ against u for (c, ω) in region II of the phase diagram in Fig. 2. There are two values of y', namely, u_m and u_M identified by (33) and (31), where an equilibrium regular arc of $\mathscr{C}$ can meet with corners on the two symmetry axes. Though characteristic of the whole region II, this specific graph was drawn for $c = \frac{\sqrt{3}}{2}$ and $\omega = 5$.

$$u_m := \sqrt{\frac{1}{\chi_1} - 1}, \tag{33}$$

identifies the value of y' where an equilibrium regular arc can meet a corner of the y axis. These corners together with those on the x axis, where $y' = u_M$, make the equilibrium shape of the drop resemble a diamond [see Fig. 17b in the main paper]. Precisely, as above, one could try and extend an equilibrium regular arc of $\mathscr{C}$ also for $y' < u_m$, but again the lack of monotonicity of Φ for $0 < u < u_m$ is likely to bring $\mathscr{C}$ in the realm of metastability.

Figure 5 illustrates the typical graph of Φ against u in region III of the phase diagram in Fig. 2. Here Φ is monotonic and so y' grows steadily from nought to infinity as ξ traverses the interval $[0, \xi_\infty]$, with ξ_∞ still given by (32). The whole curve $\mathscr{C}$ is smooth at equilibrium, as shown for example by Fig. 17c in the main paper.

By (28), for $\frac{1}{\sqrt{2}} \leqq c \leqq 1$, the aspect ratio ρ of the extensions of the drop along $\boldsymbol{n}$ and orthogonally to $\boldsymbol{n}$ can be expressed as

$$\rho(c, \omega) := \left|\frac{\Phi(u_{\max}; c, \omega)}{Y(u_{\min}; c, \omega)}\right|, \tag{34}$$

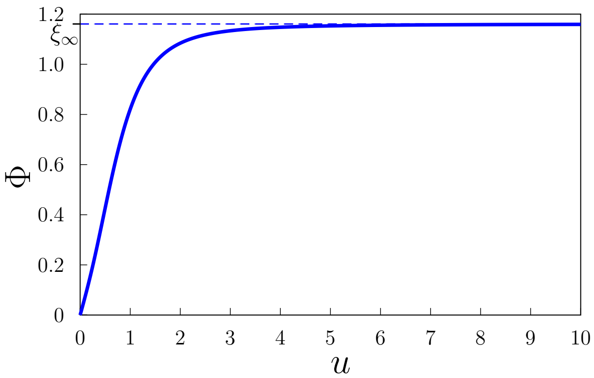

Fig. 5: The plot of the function Φ against u for (c, ω) in region III of the phase diagram in Fig. 2. Φ is monotonically increasing in the whole range $u \geqq 0$, saturating at ξ_∞, still given by (32).

where

$$u_{\max} := \begin{cases} u_M & \text{in I} \cup \text{II}, \\ \infty & \text{in III}, \end{cases} \qquad u_{\min} := \begin{cases} 0 & \text{in I} \cup \text{III}, \\ u_m & \text{in II}. \end{cases} \tag{35}$$

As a consequence of (30), ρ is easily seen to satisfy equation (16) in the main text.